Drug Design, Development and Therapy

Dovepress
Taylor & Francis Group

Open Access Full Text Article

ORIGINAL RESEARCH

# DAPT Mitigates Osteoarthritic Cartilage Degeneration and Enhances Articular Repair Through Targeted Modulation of the Gucy1a3 and Notch Signaling Axis

Xiaoyan Zheng[1,2,*], Rui Lin[1,3,*], Shan Huang[4,5], Qiqing Zeng[4,5], Xiang Gao[6], Yuyu Liu[4], Yanzhi Liu[1,3]

[1]Institute of Clinical Medicine, Zhanjiang Central Hospital, Guangdong Medical University (Central People's Hospital of Zhanjiang), Zhanjiang, 524045, People's Republic of China; [2]Department of Pharmacy, Zhanjiang Central Hospital, Guangdong Medical University (Central People's Hospital of Zhanjiang), Zhanjiang, 524045, People's Republic of China; [3]Key Laboratory of Traditional Chinese Medicine for the Prevention and Treatment of Infectious Diseases, Zhanjiang Central Hospital, Guangdong Medical University (Central People's Hospital of Zhanjiang), Zhanjiang, 524045, People's Republic of China; [4]Marine Medical Research Institute of Zhanjiang, School of Ocean and Tropical Medicine, Guangdong Medical University, Zhanjiang, 524023, People's Republic of China; [5]School of Pharmacy, Guangdong Medical University, Zhanjiang, 524023, People's Republic of China; [6]Stem Cell Research and Cellular Therapy Center, The Affiliated Hospital of Guangdong Medical University, Zhanjiang, 524001, People's Republic of China

*These authors contributed equally to this work

Correspondence: Yanzhi Liu, Institute of Clinical Medicine, Zhanjiang Central Hospital, Guangdong Medical University (Central People's Hospital of Zhanjiang), No. 236, Yuanzhu Road, Zhangjiang City, Guangdong Province, 524045, People's Republic of China, Tel +86 0759 3157875, Email liuyanzhi@gdmu.edu.cn; Yuyu Liu, Marine Medical Research Institute of Zhanjiang, School of Ocean and Tropical Medicine, Guangdong Medical University, No. 2, Wenmingdong Road, Zhangjiang City, Guangdong Province, 524023, People's Republic of China, Tel +86 0759 2387984, Email liuyuyu77@163.com



**Background:** While Nitric oxide (NO) and Notch signaling pathways are implicated in osteoarthritis (OA) progression, their functional interplay remains largely unexplored. We hypothesized that Gucy1a3 (sGCα1) functions as a non-canonical soluble sensor, bridging nitrosative stress to pathological Notch activation.

**Methods:** To test the hypothesis that Gucy1a3 mediates NO-Notch crosstalk, we used both sodium nitroprusside (SNP)-stimulated chondrocytes and a rat medial meniscus resection model. Mechanistic hierarchy was analyzed via Gucy1a3 siRNA knockdown and the Notch inhibitor DAPT. Additionally, the capacity of DAPT to modulate chondrogenic lineage commitment was evaluated in rat bone marrow mesenchymal stem cells (BMSCs).

**Results:** DAPT reversed SNP-induced catabolism in chondrocytes, suppressing Notch components (Notch1, Jagged1) and inflammatory markers (iNOS, MMP13) while restoring anabolic gene expression. Crucially, DAPT suppressed Gucy1a3 expression, breaking a reciprocal positive feedback loop (NO-Gucy1a3-Notch). Although Gucy1a3 knockdown phenocopied the anti-inflammatory signature of DAPT, DAPT uniquely activated the chondrogenic differentiation of BMSCs. In preclinical models, intra-articular delivery of DAPT effectively safeguarded joint homeostasis by reducing subchondral bone deterioration and decreasing cartilage degeneration.

**Conclusion:** This study identifies Gucy1a3 as a mediator that transduces inflammatory nitric oxide signals to activate Notch. DAPT exerts therapeutic effects by inhibiting Gucy1a3-mediated catabolism in chondrocytes and promoting the differentiation of BMSCs. Although these findings are currently limited to in vitro and rodent models, targeting this signaling axis offers a potential strategy for developing disease-modifying osteoarthritis drugs.

**Keywords:** osteoarthritis, Gucy1a3, notch signaling, DAPT, cartilage

## Introduction

Osteoarthritis (OA) progresses not merely because cartilage wears down, but because its intrinsic repair capacity fails under chronic inflammatory stress. Central to this degeneration is nitric oxide (NO), a key inflammatory mediator that

https://doi.org/10.2147/DDDT.S599941
Received: 2 March 2026
Accepted: 2 May 2026
Published: 14 May 2026

**Graphical Abstract**

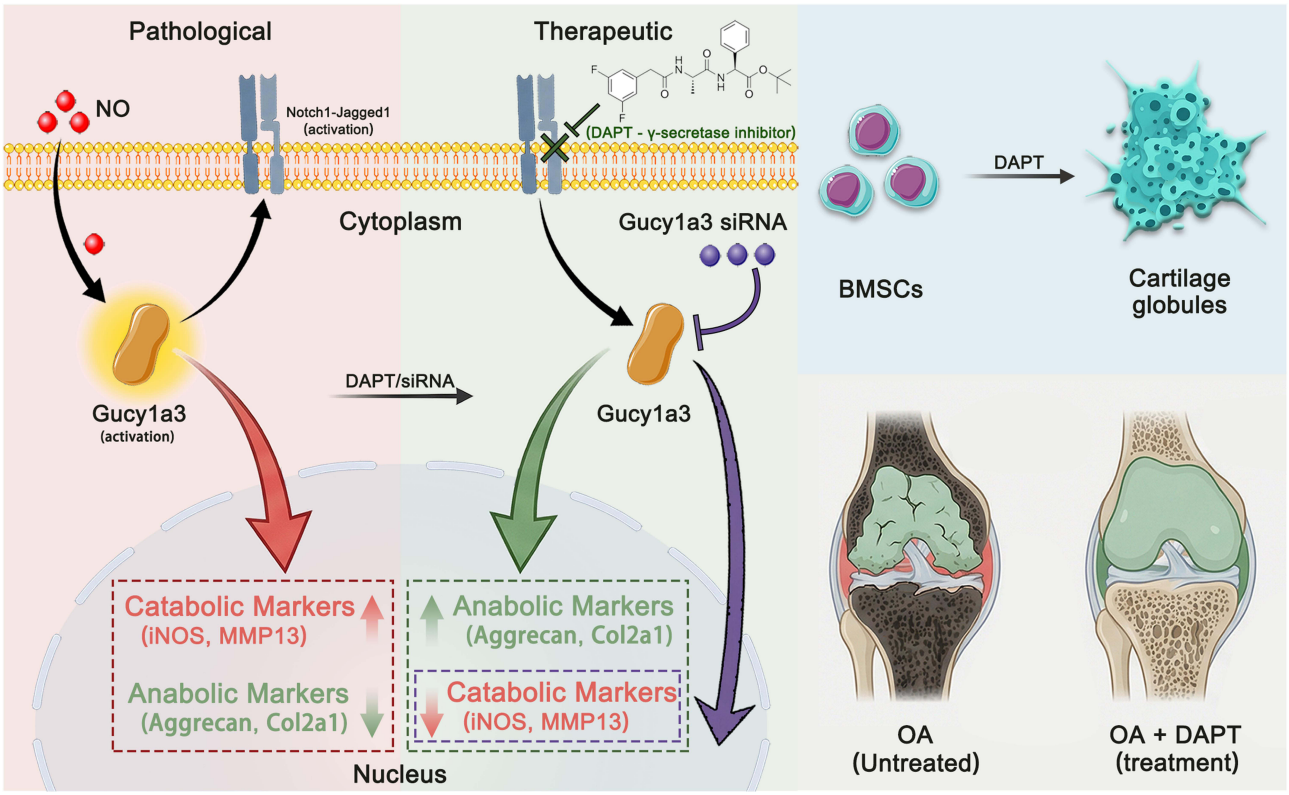


shifts chondrocytes into a catabolic state, suppressing matrix synthesis and inducing apoptosis.[1–3] Despite extensive clinical use, current OA treatments mainly relieve pain and inflammation and fail to reverse structural deterioration. Alternative therapeutic strategies, including herbal medicines, demonstrate chondroprotective efficacy by modulating specific intracellular signaling networks. For example, targeted inhibition of the PI3K/AKT pathway using specific herbal formulations prevents excessive mitophagy of chondrocytes[4] and attenuates inflammation and apoptosis.[5] Developing more efficacious disease-modifying therapies necessitates a deeper interrogation of how nitric oxide-dependent inflammatory environments predispose the articular matrix to structural failure.

Accumulating evidence points to aberrant activation of Notch signaling as a critical node in this process.[6,7] While Notch signaling is essential for joint development, its sustained overactivation is a hallmark of OA,[8] driving matrix metalloproteinase (MMP) expression, thereby accelerating extracellular matrix degradation and cartilage breakdown.[9,10] Studies in cancer biology have shown that NO can function upstream of Notch activation.[11–13] However, a fundamental mechanistic gap remains unresolved in cartilage biology: how does a diffusible gas initiate activation of Notch, a receptor classically restricted to cell-to-cell contact via canonical juxtacrine interactions? Clarifying this transition from a soluble inflammatory signal to a membrane-bound receptor pathway is essential for understanding OA progression and identifying actionable therapeutic targets. Conventional models of Notch activation rely strictly on the engagement of membrane-bound ligands (eg, Jagged or Delta-like) on adjacent cells,[7,14] leaving this atypical, soluble-phase activation largely unexplored. Bridging this gap is critical for identifying actionable therapeutic targets that can uncouple inflammation from structural degradation.

The soluble guanylate cyclase (sGC) heterodimer, specifically its α1 subunit encoded by *Gucy1a3*, serves as the primary physiological receptor for bioavailable NO. Although sGC function is well established in vascular homeostasis, its specific role in osteoarthritis pathogenesis remains largely underexplored. Gucy1a3 shares a reciprocal regulatory relationship with the Notch pathway. Evidence from cardiovascular research indicates that Gucy1a3 is a direct transcriptional target of Notch

signaling, where Notch activation upregulates sGC expression via RBPJ-dependent mechanisms.[15] This finding suggests that Gucy1a3 is an integral component of the Notch signaling cascade. We hypothesize that in the osteoarthritic joint, this regulatory link forms a positive feedback loop where Gucy1a3 acts as the initial mediator that transduces nitrosative stress to activate Notch, and the resulting Notch signaling maintains high Gucy1a3 expression. This mechanism converts sGC into a pathological mediator, maintaining chondrocytes in a state of chronic inflammation and catabolism. Notch signaling maintains stem cell quiescence and inhibits lineage commitment.[16,17] In the context of OA, persistent Notch activation therefore has two detrimental consequences: it reinforces the NO-driven inflammatory and catabolic loop in chondrocytes, and it simultaneously suppresses the differentiation of mesenchymal stem cells into cartilage-forming cells. Targeting this pathway thus offers a unique opportunity to address both cartilage degeneration and impaired regeneration.

While various Notch and sGC modulators have been investigated independently for joint[10] or cardiovascular diseases,[18,19] therapeutic strategies simultaneously targeting their intersection—the NO-Gucy1a3-Notch axis—are lacking. Here, we investigate the therapeutic potential of DAPT (N-[N-(3,5-difluorophenacetyl)-L-alanyl]-S-phenylglycine t-butyl ester), a potent and highly lipophilic γ-secretase inhibitor, as a strategy to modulate this NO-Gucy1a3-Notch axis. While systemically administered γ-secretase inhibitors have been extensively evaluated in clinical trials for oncology and Alzheimer's disease,[20] their application is often limited by gastrointestinal toxicity. Consequently, DAPT is predominantly utilized as a precise preclinical tool. By employing intra-articular delivery to circumvent systemic toxicity, we hypothesize that DAPT-mediated Notch inhibition interacts with Gucy1a3 signaling to disrupt the catabolic program in chondrocytes, while simultaneously activating the dormant chondrogenic differentiation potential of mesenchymal stem cells. By defining the critical role of the NO-Gucy1a3-Notch axis in chondrocyte degeneration, this study aims to validate a dual-action strategy that not only suppresses degeneration but actively restores joint homeostasis, offering a mechanistic framework for future preclinical development of osteoarthritis therapeutics.

# Materials and Methods

## Materials, Animals, and Cell Lines

High-glucose DMEM, fetal bovine serum (FBS), and DAPI were purchased from Thermo Fisher Scientific (Waltham, MA, USA). The γ-secretase inhibitor DAPT was obtained from MedChemExpress (Monmouth Junction, NJ, USA). Sodium nitroprusside (SNP), sodium pentobarbital, and paraformaldehyde were sourced from Sigma-Aldrich (St. Louis, MO, USA). Gucy1a3-specific siRNAs were synthesized by GenePharma Suzhou, China).

Eighteen specific pathogen-free (SPF) male Sprague-Dawley (SD) rats (300 ± 20 g) were procured from the Guangdong Laboratory Animals Monitoring Institute (Guangzhou, China). The C28/I2 human chondrocyte cell line was purchased from Shanghai Zeye Biotechnology Co., Ltd. (Shanghai, China). C28/I2 is a well-established immortalized human chondrocyte line. Rat bone marrow mesenchymal stem cells (BMSCs) were obtained from Cyagen Biosciences Inc. (Shanghai, China).

## Ethics Approval and Consent to Participate

Animal experiments were conducted in compliance with the Guide for the Care and Use of Laboratory Animals (National and Guangdong Laboratory Animal Monitoring Institutes, China). The protocol was approved by the Experimental Animal Ethics Committee of the Affiliated Hospital of Guangdong Medical University (Permit No. AHGDMU-LAC-I(1)-2208-A029).

## Cell Culture and Treatment

C28/I2 chondrocytes were cultured in high-glucose DMEM supplemented with 10% FBS and antibiotics at 37°C in a humidified 5%$CO_2$ atmosphere. For Sodium Nitroprusside (SNP) and DAPT (Cat# HY-13027, MedChemExpress) treatments, compounds were dissolved directly in the culture medium. For BMSC experiments, DAPT was incorporated into the chondrogenic induction medium.

## Cell Viability Assay

C28/I2 cells were seeded in 96-well plates and exposed to specific concentrations of SNP and DAPT for 24 hours. Cell viability was quantified using the Cell Counting Kit-8 (CCK-8; Beyotime, Shanghai) following the manufacturer's instructions to optimize intervention concentrations.

## siRNA Transfection

C28/I2 chondrocytes were transfected at ~80% confluence using Lipofectamine® 3000 (Invitrogen) and Gucy1a3-specific siRNA (5 μg). Transfection complexes were prepared in Opti-MEM (or serum-free medium) and incubated with cells for 4–6 hours, after which the medium was replaced with complete medium with or without drug supplementation. Cells were harvested 24 hours post-treatment for RNA extraction and 48 hours post-treatment for protein analysis. To maximize transparency, the specific siRNA sequences targeting human Gucy1a3 used in this study were: Gucy1a3-Homo-1201 (Sense: 5'-GCUCACGUAUUAUAUGAAATT-3'; Antisense: 5'-UUUCAUAUAAUACGUGAGCTT-3'), Gucy1a3-Homo -2339 (Sense: 5'-CUCUGGCUAACAAAUUUGATT-3'; Antisense: 5'-UCAAAUUUGUUAGCCAGAGTT-3'), Gucy1a3-Homo-1545 (Sense: 5'-GAUCAUGACUAUGUUGAAUTT-3'; Antisense: 5'-AUUCAACAUAGUCAUGAUCTT-3'), and Gucy1a3-Homo-1599 (Sense: 5'-CAGGUCAAGUUCCUAACGATT-3'; Antisense: 5'-UCGUUAGGAACUUGACCUGTT-3').

## Quantitative Real-Time PCR (qPCR)

Total RNA was extracted using TRIzol® reagent (Takara), and cDNA was synthesized using the PrimeScript™ RT Master Mix (Takara). Gene expression was quantified on an ABI 7500 System using SYBR® Premix Ex Taq™ II. Target gene expression (*Notch1, Jagged1, TNFα, Gucy1a3, Aggrecan, Col2a1, iNOS, MMP13, IL6, ADAMTS5* and *IL-1β*) was normalized to GAPDH using the ($2^{-\Delta\Delta Ct}$) method, which calculates the relative fold change in gene expression by comparing the threshold cycle (Ct) of the target gene to that of the reference gene across experimental and control groups. The PCR cycling conditions were: initial denaturation at 95°C for 30 sec, followed by 40 cycles of denaturation at 95°C for 5 sec and annealing/extension at 60°C for 34 sec. Primer sequences used in RT-qPCR are listed in Supplementary Table S1.

## Western Blotting

Proteins were extracted using RIPA buffer (Cat# P0013C, Beyotime Biotechnology, Shanghai, China), separated by SDS-PAGE, and transferred to PVDF membranes (Cat# FFP77, Beyotime Biotechnology). After blocking, membranes were incubated overnight at 4°C with primary antibodies against Collagen II (Cat# ab188570, Abcam, Cambridge, MA, USA), Aggrecan (Cat# ab3778, Abcam) and Gucy1a3 (Cat# 12605-1-AP, Wuhan Sanying). Bands were detected using HRP-conjugated secondary antibodies (Cat# A21020, Abbkine Scientific Co., Ltd., Redlands, CA, USA) and visualized with the FluorChem® Q System (ProteinSimple, San Jose, CA, USA). Protein expression levels were quantified and normalized using ImageJ software (National Institutes of Health, Bethesda, MD, USA).

## Chondrogenic Differentiation Assay

BMSCs were cultured to ≥90% confluence and switched to chondrogenic induction medium, renewed every 48 hours. After 14 days, differentiation was evaluated via Alcian Blue staining. Briefly, cells were fixed in 4% paraformaldehyde, acidified with 0.1 M HCl, and stained overnight. Cartilaginous globules were imaged under a light microscope.

## Establishment of OA Model

Eighteen male Sprague-Dawley (SD) rats were randomized into three groups (n=6/group): Control (Sham), OA (medial meniscectomy + vehicle), and DAPT (medial meniscectomy + 2.5 μM DAPT).

Surgical anesthesia was induced via an intraperitoneal (IP) injection of sodium pentobarbital (50 mg/kg).[21] The right knee joint was exposed through a longitudinal incision, and the medial meniscus was resected to establish the OA model. The 2.5 μM DAPT working solution was prepared by diluting a 25 mM stock (dissolved in DMSO) at a ratio of 1:10,000 in saline, resulting in a final dimethyl sulfoxide (DMSO) concentration of 0.01% (v/v) per injection. This specific concentration and the administration regimen (2.5 μM, 10 μL/knee, twice weekly for 4 weeks) were adopted from a validated in vivo protocol for intra-articular Notch inhibition as previously reported.[10] To control for solvent effects, the OA group received an equivalent volume of vehicle (DMSO diluted in saline).[10]

At the end of the 4-week experimental period, all rats were euthanized in strict compliance with the AVMA Guidelines for the Euthanasia of Animals (2020 Edition).[22] Specifically, the rats were deeply anesthetized with inhaled isoflurane (induced at 4–5% and maintained at 2–3% in oxygen). Once a surgical plane of anesthesia was confirmed by

the complete loss of the pedal withdrawal reflex, terminal blood sample collection was performed via cardiac puncture, leading to death by exsanguination. Death was further confirmed by the permanent cessation of respiration and heartbeat prior to tissue harvest, supplemented by a secondary physical confirmation (cervical dislocation). All procedures were designed to minimize animal distress and were approved by the local Institutional Animal Care and Use Committee. Hindlimb specimens were subsequently collected for downstream analyses.

## Micro-CT Analysis

Fixed hindlimbs were scanned using a Viva CT40 system (Scanco Medical) with the following high-resolution parameters: image matrix size 2048 × 2048, integration time 200 ms, energy 70 kVp, intensity 114 μA, power 8 W. Scanning was conducted over a 15-mm region using a calibration phantom of 1200 mg hydroxyapatite (HA)/$cm^3$. A region of interest (ROI) was defined to quantify bone microarchitecture parameters, including Bone Volume/Tissue Volume (BV/TV), Bone Surface area/Tissue Volume (BS/TV), Trabecular Number (Tb.N), Thickness (Tb.Th), Separation (Tb.Sp), and Pattern Factor (Tb.Pf). 3D reconstructions were generated using CTvox software.

## Histological Evaluation

Femora were decalcified in 12% EDTA for 4 weeks. Decalcified specimens were then sequentially dehydrated and cleared through a graded ethanol series: 70% ethanol (24 h), 80% ethanol (12 h), 90% ethanol (2 h), and two changes of 100% ethanol (1 h each). Subsequent clearing was performed in xylene for 40 minutes. Tissues were infiltrated with paraffin wax: soft wax (2 h) followed by hard wax (2 h), and finally embedded in paraffin blocks. Sections (5 μm) were stained with Hematoxylin and Eosin (H&E) (Cat# G1120, Solarbio, Beijing, China) and Safranin O-Fast Green (Cat# G1371, Solarbio, Beijing, China). Cartilage degeneration was graded using the Mankin scoring system.[23,24]

## Immunofluorescence

Antigen retrieval was performed with proteinase K. Sections were blocked with 5% BSA + 0.3% Triton X-100 and incubated overnight with anti-Collagen II antibody (ab3092, 1:100, Abcam), followed by Alexa Fluor® 647-conjugated secondary antibody (ab150115, 1:200, Abcam). Nuclei were counterstained with DAPI. Images were captured using fluorescence microscopy.

## Statistical Analysis

Data were visualized using GraphPad Prism 8.0, and statistical analyses were performed using SPSS 19.0. The exact sample size (n, representing independent biological replicates) for each experiment is specified in the figure legends.

For datasets with n≥5 per group (eg, in vivo experiments): Data distribution and variance homogeneity were evaluated using the Shapiro–Wilk test and Levene's test, respectively. For normally distributed data with equal variances, differences between two groups were analyzed using an independent-samples *t*-test, and multiple groups were compared using a standard one-way ANOVA followed by Tukey's post hoc test to correct for multiple comparisons and control type I error. In instances where the assumption of homoscedasticity was violated, Welch's *t*-test or Welch's one-way ANOVA was employed. Subsequent multiple comparisons were performed using the Games-Howell post-hoc procedure to account for unequal variances.

For datasets with n<5 per group (eg, in vitro qPCR and Western blot experiments): In strict accordance with robust statistical guidelines, traditional parametric tests relying on distributional assumptions were waived. Instead, bootstrap resampling (1000 iterations, percentile method) was used as a distribution-free optimized alternative to evaluate statistical significance with 95% confidence intervals.

Statistical significance was determined exclusively by the bootstrap-derived 95% confidence intervals (CI) of the mean differences. A difference was considered statistically significant (equivalent to $P<0.05$) when the upper and lower bounds of the 95% CI shared the same sign (ie, strictly excluded zero). The exact bootstrap-derived 95% CIs and mean differences for all n=3 in vitro experiments are comprehensively detailed in Supplementary Tables S2–S6.

# Results

## DAPT Restores SNP-Induced Cartilage Damage in Chondrocytes by Modulating Notch Signaling

To establish a reliable chondrocyte injury model, C28 cells were first exposed to varying concentrations of sodium nitroprusside (SNP) for 24 hours. The CCK-8 assay showed that 0.5 mM SNP significantly reduced cell viability by 19.08% ($P < 0.05$; Figure 1A), inducing a robust yet non-lethal catabolic stress suitable for downstream evaluation. RT-qPCR analysis confirmed that this 0.5 mM SNP treatment significantly upregulated *Jagged1, Notch1, iNOS*, and *Gucy1a3* mRNA levels by 19.51% ($P < 0.05$), 33.58% ($P < 0.05$), 23.01% ($P < 0.05$), and 44.35% ($P < 0.05$), respectively (Figure 1B).

We evaluated the effect of DAPT on the injury model using a dose gradient assay. The 25 μM DAPT concentration provided optimal cytoprotection without basal toxicity, whereas higher concentrations including 50 μM decreased cell viability likely due to cumulative solvent toxicity. In a subsequent independent assay batch, 0.5 mM SNP reduced cell viability by 31.6% ($P < 0.01$). Cotreatment with 25 μM DAPT recovered chondrocyte viability by 24.87% ($P < 0.05$; Figure 1C). We utilized 25 μM DAPT for all subsequent in vitro assays based on these viability assessments.

RT-qPCR showed that DAPT intervention significantly suppressed SNP-induced upregulation of *Notch1, Jagged1, TNFα, Gucy1a3, iNOS, MMP13* and *IL-1β* by 45.89% ($P < 0.05$), 35.63% ($P < 0.05$), 46.82% ($P < 0.05$), 12.40% ($P < 0.05$), 11.27% ($P < 0.05$), 19.82% ($P < 0.05$), and 78.60% ($P < 0.05$), respectively. Conversely, DAPT markedly increased *Aggrecan* and *Col2a1* by 36.13% ($P < 0.05$) and 32.32% ($P < 0.05$), respectively (Figure 1D–L). The exact bootstrap-

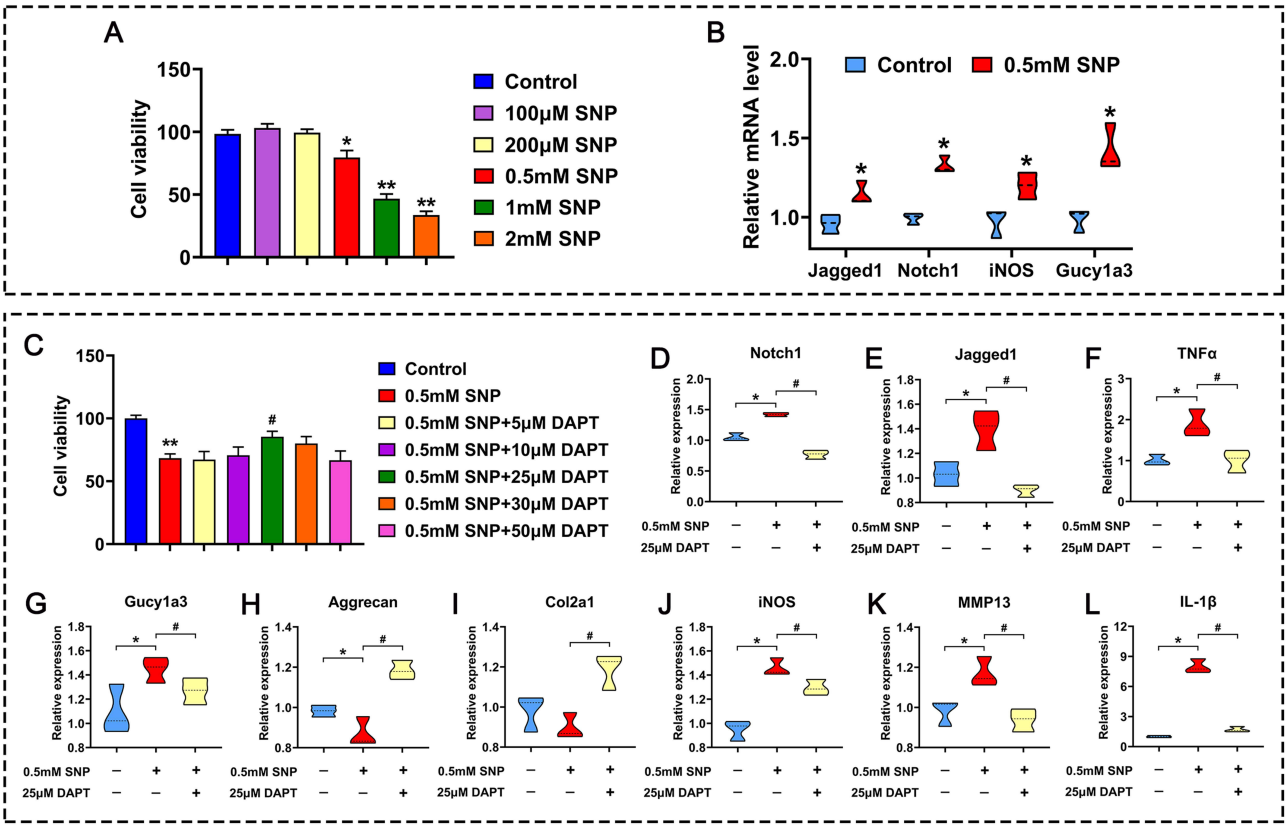


**Figure 1** DAPT protects C28 chondrocytes against SNP-induced cytotoxicity and catabolism. (**A**) Cell viability assessed by CCK-8 assay following treatment with increasing concentrations of SNP. (**B**) RT-qPCR analysis of *Jagged1, Notch1, iNOS*, and *Gucy1a3* mRNA levels in cells treated with 0.5 mM SNP. (**C**) Rescue of cell viability by DAPT in SNP-injured chondrocytes. (**D**–**L**) RT-qPCR quantification of *Notch1, Jagged1, TNFα, Gucy1a3, Aggrecan, Col2a1, iNOS, MMP13* and *IL-1β* expression in cells co-treated with 0.5 mM SNP and 25 μM DAPT. All data are presented as mean ± SD. For CCK-8 assays (**A** and **C**), n=6 independent biological replicates. For RT-qPCR analyses (**B** and **D**–**L**), n=3 independent biological replicates. Due to the small sample size (**B** and **D**–**L**, n=3), statistical significance was determined using bootstrap resampling (1000 iterations, percentile method) based on the exclusion of zero from the 95% confidence interval (CI). Detailed bootstrap 95% CIs for these comparisons are provided in Supplementary Table S2. **P*<0.05, ***P*<0.01 vs. Control group; $^{\#}P$<0.05 vs. SNP group.


https://doi.org/10.2147/DDDT.S599941

derived 95% confidence intervals and mean differences confirming statistical significance for all corresponding n=3 in vitro comparisons are detailed in Supplementary Table S2.

## DAPT Promotes Chondrocyte Anabolism and Differentiation by Inhibiting Gucy1a3

In C28 cells, 25 μM DAPT significantly increased ACAN and Collagen II protein levels by 78.13% ($P < 0.05$) and 61.38% ($P < 0.05$), while decreasing Gucy1a3 protein by 48.59% ($P < 0.05$) (Figure 2A). Consistent with this, RT-qPCR showed DAPT markedly boosted *Aggrecan* and *Col2a1* mRNA levels by 168.51% ($P < 0.05$) and 192.09% ($P < 0.05$), while suppressing *Gucy1a3, iNOS*, and *MMP13* by 81.45% ($P < 0.05$), 83.77% ($P < 0.05$), and 83.08% ($P < 0.05$) (Figure 2B). Detailed 95% confidence intervals from the bootstrap resampling analyses verifying these differences are provided in Supplementary Table S3.

In BMSCs, 25 μM DAPT effectively drove chondrogenic differentiation. Alcian Blue staining showed DAPT significantly increased the number and area of cartilage globules by 240% ($P < 0.01$) and 243.91% ($P < 0.001$), respectively (Figure 3).

## DAPT Protects Against Cartilage Damage via the Gucy1a3/Notch Axis

To validate the role of Gucy1a3, we selected the most effective siRNA construct (Gucy1a3(-)-H-1545) (Figure 4A). In Gucy1a3 knockdown C28 cells, *Jagged1, Notch1, iNOS*, and *Gucy1a3* mRNA levels were significantly reduced by 24.21% ($P < 0.05$), 27.97% ($P < 0.05$), 51.86% ($P < 0.05$), and 42.15% ($P < 0.05$) (Figure 4B). Additionally, Gucy1a3 knockdown suppressed *IL-6* and *ADAMTS5* expression by 75.22% ($P < 0.05$) and 68.16% ($P < 0.05$) compared to the negative control (Figure 4C).

Crucially, SNP effectively reversed the effects of Gucy1a3 knockdown. In knockdown cells, SNP robustly upregulated *Gucy1a3, Notch1, IL-6*, and *ADAMTS5* by 245.82% ($P < 0.05$), 347.13% ($P < 0.05$), 131.39% ($P < 0.05$), and 267.19% ($P < 0.05$) (Figure 4C). Concurrently, ACAN and Collagen II protein levels were reduced by 51.88% ($P < 0.05$) and 50.03% ($P < 0.05$) (Figure 4D).

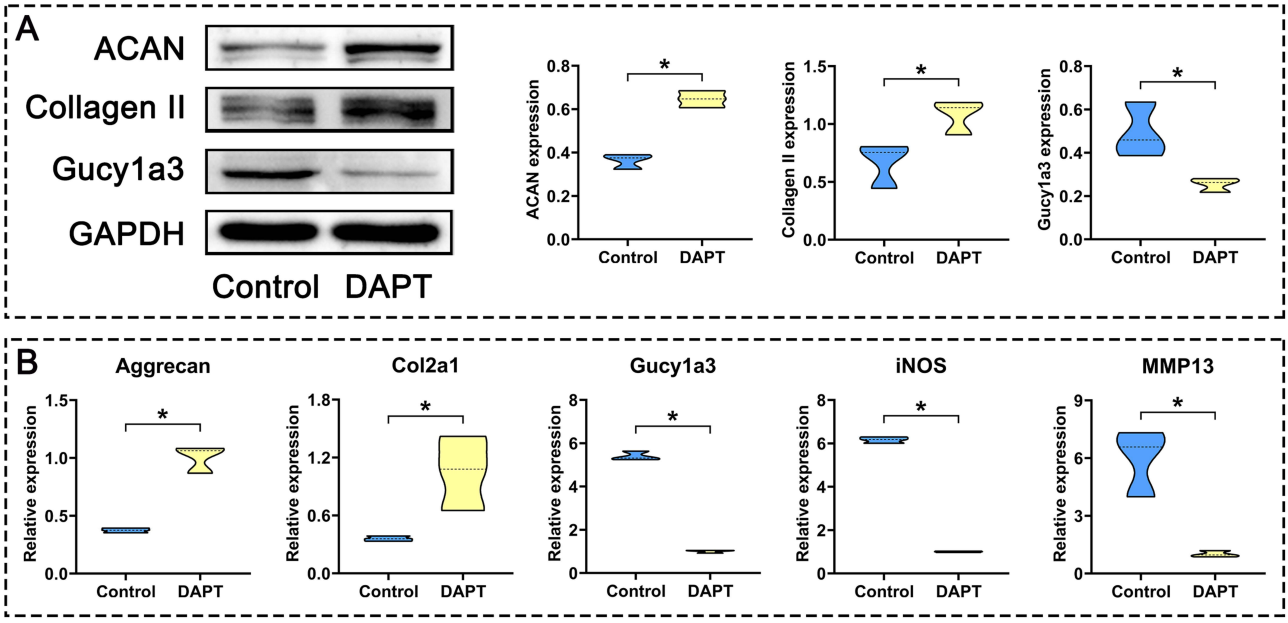


**Figure 2** DAPT promotes anabolic markers and suppresses Gucy1a3 expression in C28 chondrocytes. (**A**) Western blot of ACAN, Collagen II, and Gucy1a3 protein levels following 25 μM DAPT treatment. (**B**) RT-qPCR quantification of *Aggrecan, Col2a1, Gucy1a3, iNOS*, and *MMP13* mRNA expression in C28 cells treated with 25 μM DAPT. All data are presented as mean ± SD (n=3 independent biological replicates). Due to the small sample size, statistical significance was determined using bootstrap resampling (1000 iterations, percentile method) based on the exclusion of zero from the 95% confidence interval. Detailed bootstrap 95% CIs for these comparisons are provided in Supplementary Table S3. *$P$<0.05 vs. Control group.


https://doi.org/10.2147/DDDT.S599941

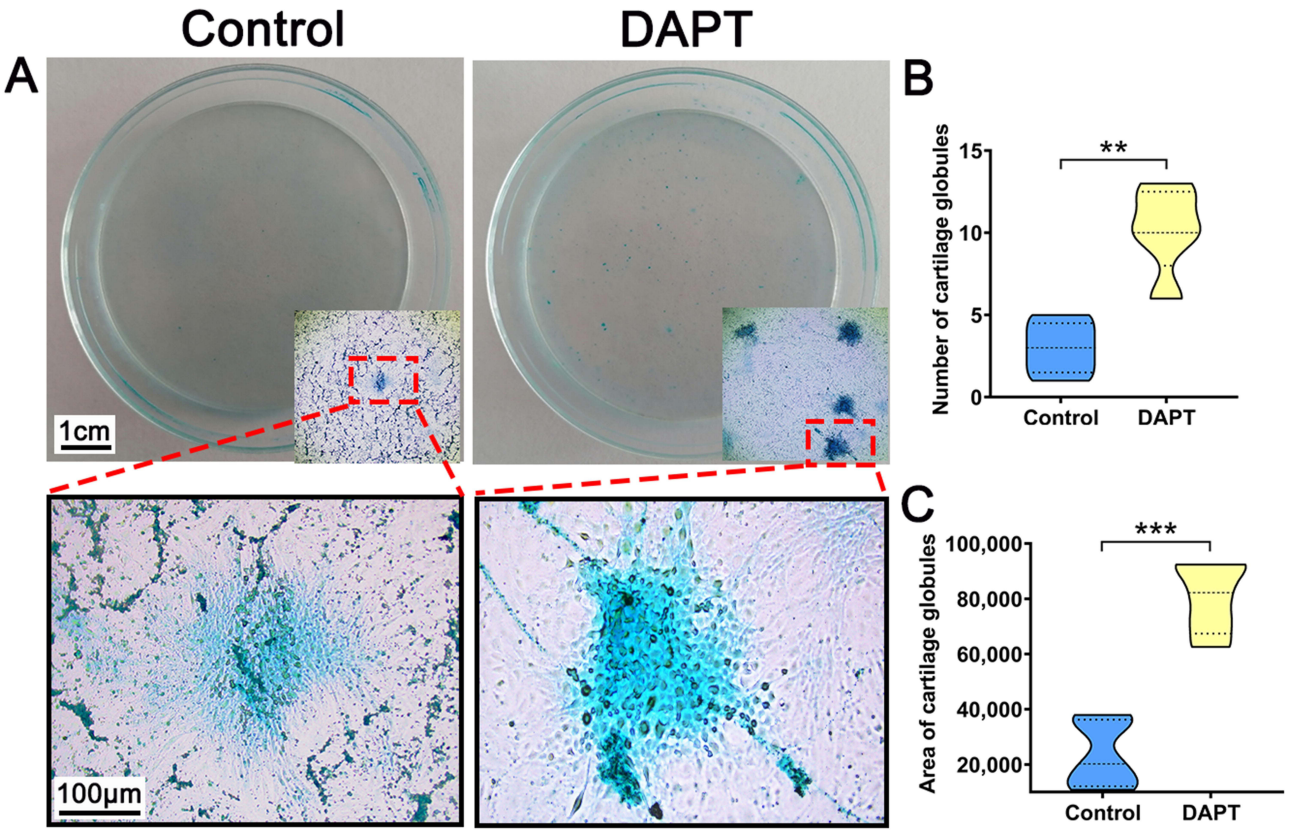


**Figure 3** DAPT enhances chondrogenic differentiation in BMSCs. (**A**) Representative images of Alcian Blue staining in bone marrow mesenchymal stem cells (BMSCs) following chondrogenic induction with or without 25 μM DAPT. Note: The red dashed box shows the zoomed image. (**B** and **C**) Quantification of the number (**B**) and area (**C**) of Alcian Blue-positive cartilage globules. All data are presented as mean ± SD (n=5 independent biological replicates). ***P*<0.01, ****P*<0.001 vs. Control group.

We then examined the effect of adding DAPT to this system. RT-qPCR showed that DAPT countered the SNP effect, downregulating *Gucy1a3, Jagged1, Notch1*, and *iNOS* by 28.97% ($P < 0.05$), 26.23% ($P < 0.05$), 15.68% ($P < 0.05$), and 19.77% ($P < 0.05$) (Figure 4E). Comprehensive bootstrap 95% confidence intervals supporting the statistical significance of the *Gucy1a3* knockdown and subsequent DAPT rescue experiments (n=3) are cataloged in Supplementary Tables S4–S6.

## DAPT Improves Joint Structure in OA Rats

The grouping and treatment of the in vivo experiments are shown in Figure 5A. Histologically, DAPT intervention substantially reduced cartilage damage and enhanced Collagen II expression (Figure 5B). Mankin scoring showed a 300% increase ($P < 0.001$) in OA rats versus Sham, which was significantly lowered by 32.81% ($P < 0.01$) with DAPT treatment (Figure 5C).

Micro-CT analysis revealed significant bone loss in the OA group (Figure 6A). Quantitative metrics showed reduced BV/TV, BS/TV, Tb.N, and Tb.Th by 46.68% ($P < 0.001$), 17.24%, 27.47%, and 28.01% ($P < 0.05$), alongside increased Tb.Sp and Tb.Pf by 66.42% ($P < 0.01$) and 159.11% (Figure 6B). DAPT treatment markedly prevented this bone loss. Compared to the OA group, DAPT significantly increased BV/TV, BS/TV, Tb.N, and Tb.Th by 31.45% ($P < 0.01$), 30.10% ($P < 0.01$), 33.52% ($P < 0.001$), and 2.50%, while reducing Tb.Sp and Tb.Pf by 37.19% ($P < 0.001$) and 5.32% (Figure 6B).

# Discussion

In this study, the results revealed that DAPT functions as a potent disease-modifying osteoarthritis drug candidate by targeting the Gucy1a3/Notch signaling axis. In vitro, DAPT treatment not only rescued chondrocytes from SNP-induced

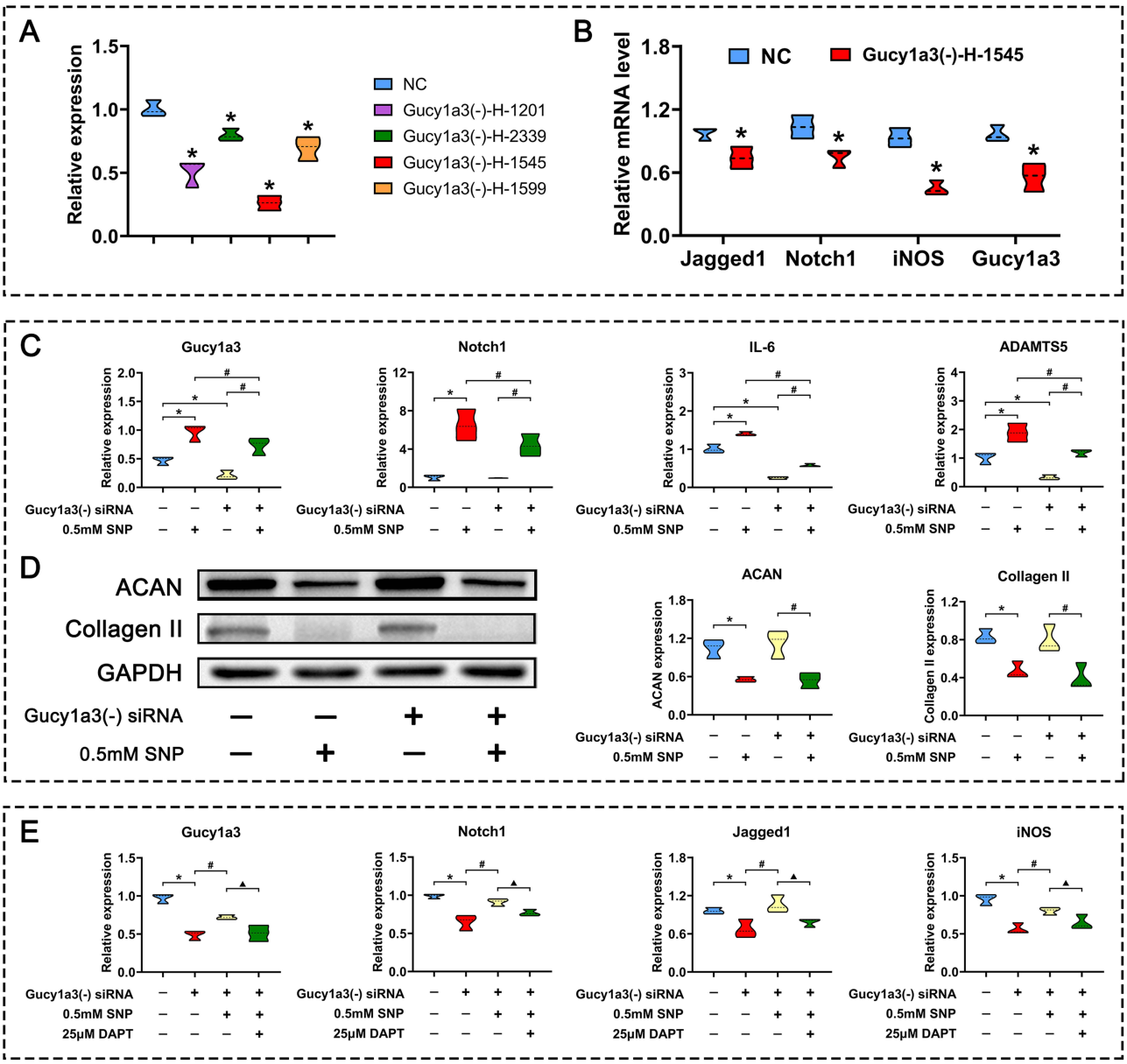


**Figure 4** DAPT and *Gucy1a3* knockdown modulate Notch signaling and matrix homeostasis under nitrosative stress. (**A**) RT-qPCR screening of *Gucy1a3* siRNA knockdown efficiency. (**B**) Impact of the optimal siRNA construct (Gucy1a3(-)-H-1545) on *Jagged1*, *Notch1*, *iNOS*, and *Gucy1a3* mRNA levels. (**C**) RT-qPCR quantification of *Gucy1a3*, *Notch1*, *IL-6*, and *ADAMTS5* expression in *Gucy1a3* knockdown cells challenged with 0.5 mM SNP. (**D**) Western blot of ACAN and Collagen II protein levels in *Gucy1a3* knockdown cells treated with 0.5 mM SNP. (**E**) Effect of 25 μM DAPT on *Gucy1a3*, *Notch1*, *Jagged1*, and *iNOS* mRNA expression in *Gucy1a3* knockdown cells co-treated with 0.5 mM SNP. All data are presented as mean ± SD (n=3 independent biological replicates). Due to the small sample size, statistical significance was determined using bootstrap resampling (1000 iterations, percentile method) based on the exclusion of zero from the 95% confidence interval. Detailed bootstrap 95% CIs for these comparisons are provided in Supplementary Tables S4–S6.*$P$<0.05 vs Negative Control (NC); #$P$<0.05 vs Gucy1a3 siRNA+SNP group; ▲$P$<0.05 vs Gucy1a3 siRNA+SNP+DAPT group.

cytotoxicity (restoring viability by 24.87%) but also actively re-established extracellular matrix homeostasis. This anabolic recovery was marked by a robust increase of Col2a1 (192.09%) and the concurrent reduction (>80%) of catabolic markers iNOS and MMP13. Beyond these cytoprotective effects, DAPT promoted chondrogenic differentiation in BMSCs, suggesting a broader regenerative potential. Mechanistically, we demonstrate that DAPT efficacy relies on breaking a pathological loop: it reverses the SNP-driven increase of Notch1 and Jagged1 while simultaneously suppressing Gucy1a3. Knockdown experiments confirmed Gucy1a3 as the critical mediator; knock down this gene replicated the anti-catabolic transcriptional profile of DAPT (downregulating Notch1, Jagged1, and iNOS). However, unlike DAPT, Gucy1a3 knock down alone failed to fully restore the anabolic markers ACAN and Collagen II. This distinction


https://doi.org/10.2147/DDDT.S599941

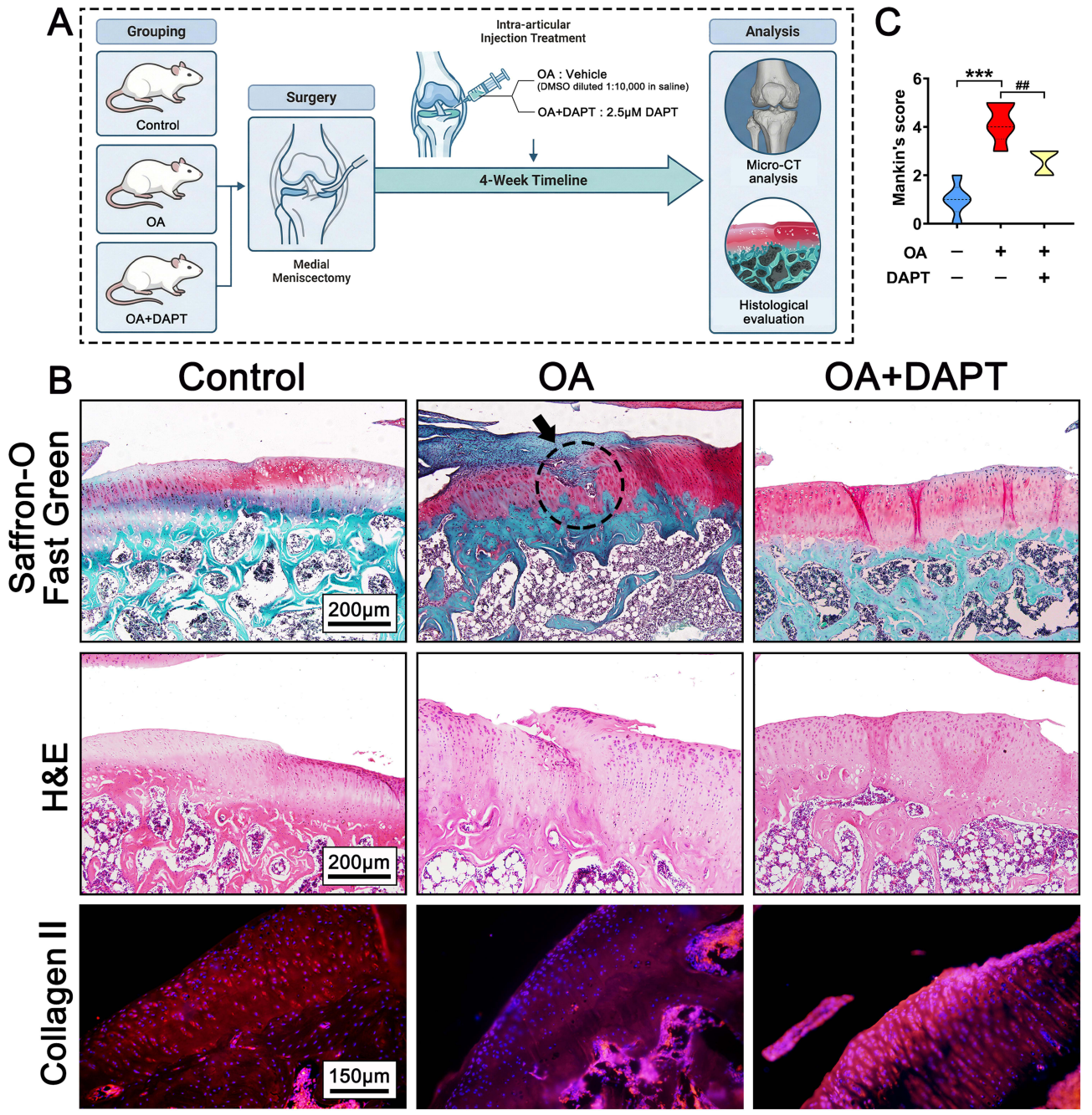


**Figure 5** Intra-articular DAPT preserves joint structural integrity and promotes cartilage repair in a rat OA model. (**A**) Schematic overview of the in vivo experimental design and treatment timeline. (**B**) Representative images of Safranin O-Fast Green staining, Hematoxylin and Eosin (H&E) staining, and Collagen II immunofluorescence in rat knee joints following 4 weeks of intra-articular 2.5μM DAPT treatment. Note: Cartilage degradation in the OA group has been clearly marked with black arrows and black dashed circular outlines. (**C**) Quantitative histopathological assessment of cartilage degeneration using the Mankin scoring system. All data are presented as mean ± SD (n=5 independent biological replicates). ***$P$<0.001 vs Control; ##$P$<0.01 vs OA group.

highlights that while Gucy1a3 primarily drives the inflammatory/catabolic arm of the pathology, DAPT exerts a dual effect: it blocks Gucy1a3-mediated catabolism and independently releases the brake on anabolism. In vivo, intra-articular DAPT significantly preserved subchondral bone microarchitecture and lowered cartilage degeneration scores. We performed micro-computed tomography to evaluate subchondral bone microarchitecture because Notch signaling regulates bone remodeling. Persistent Notch activation inhibits osteoblast differentiation[25–27] and exacerbates inflammatory bone loss.[28] DAPT penetrates the subchondral compartment and inhibits Notch signaling to promote osteoblast

 https://doi.org/10.2147/DDDT.S599941 

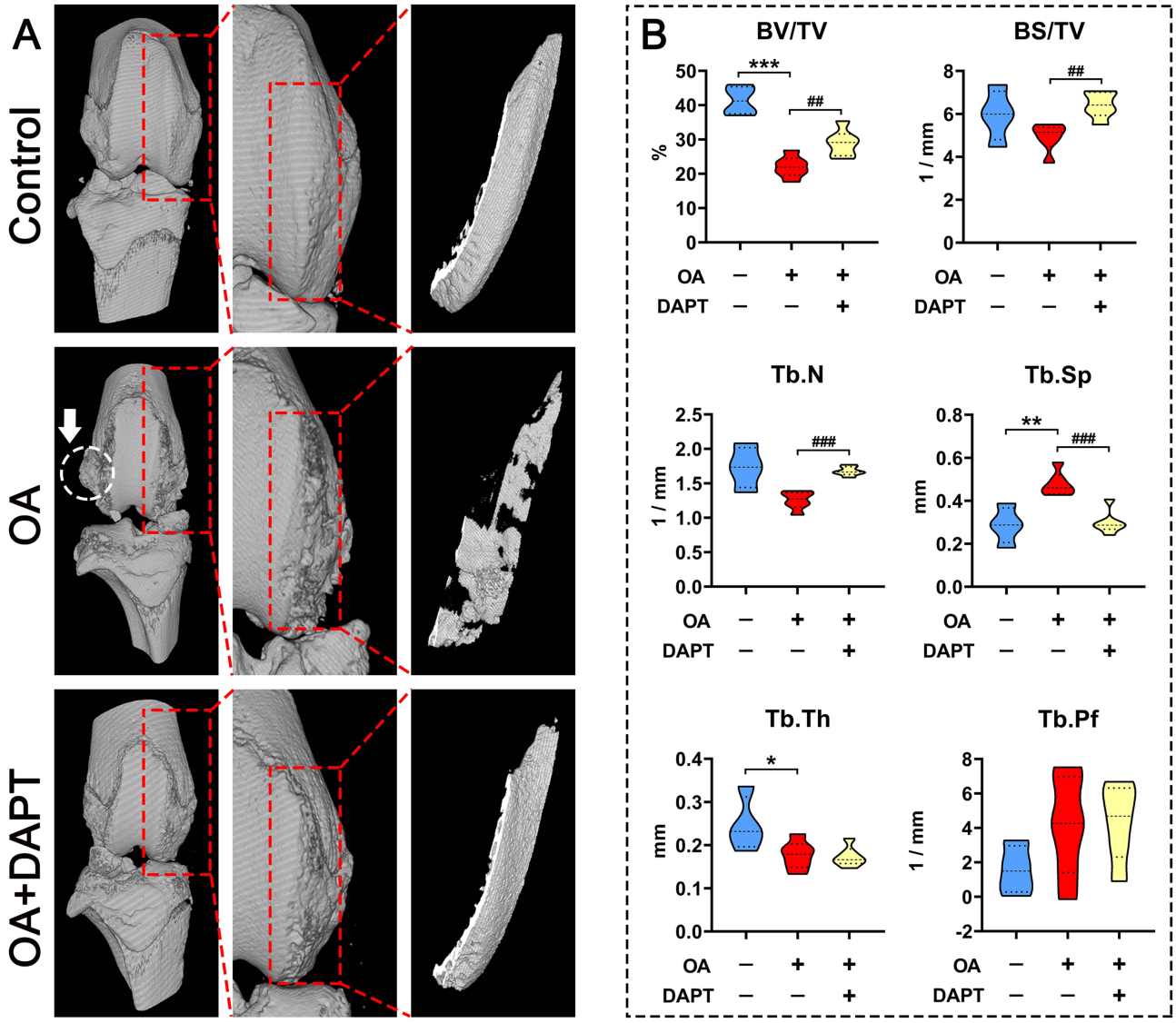


**Figure 6** Intra-articular DAPT preserves subchondral bone microarchitecture in OA rats. (**A**) Representative 3D micro-CT reconstructions of the medial femoral condyle. Note: Osteophyte formation in the OA group has been clearly marked with white arrows and white dashed circular outlines. The red dashed box shows the zoomed image. (**B**) Quantitative morphometric analysis of trabecular bone parameters: bone volume fraction (BV/TV), bone surface density (BS/TV), trabecular number (Tb.N), trabecular thickness (Tb.Th), trabecular separation (Tb.Sp), and trabecular bone pattern factor (Tb.Pf). All data are presented as mean ± SD (n=6 independent biological replicates). **P*<0.05, ***P*<0.01, ****P*<0.001 vs Control; $^{\#\#}$*P*<0.01, $^{\#\#\#}$*P*<0.001 vs OA group.

differentiation and preserve trabecular bone mass.[28] Furthermore, cartilage matrix restoration by DAPT reduces abnormal mechanical loading on the underlying bone, indirectly preventing pathological remodeling.[29] Thus, validating its translational promise, our data demonstrate that DAPT exerts comprehensive joint-protective effects by breaking the Gucy1a3-mediated Notch activation loop, highlighting its potential for clinical translation. Given the preclinical nature of this study, long-term observation is required before considering clinical translation.

Cartilage damage is central to the pathology of osteoarthritis. Nitric oxide is a known catabolic factor that drives this process by inducing chondrocyte apoptosis, matrix metalloproteinase synthesis, and proinflammatory cytokine production.[2] Persistent Notch activation occurs across multiple cell types in the osteoarthritic joint, including chondrocytes, mesenchymal stem cells,[28,30] and osteoblasts.[25–27,30] Moreover, Notch signaling is highly active in synovial macrophages, where it critically drives macrophage polarization toward the proinflammatory M1 phenotype.[31,32] In the inflammatory microenvironment, these M1-polarized synovial macrophages are the primary source of inducible nitric oxide synthase and subsequent nitric oxide production.[33–35] These activated macrophages interact extensively with surrounding joint cells through paracrine signaling to


https://doi.org/10.2147/DDDT.S599941

exacerbate osteoarthritis progression.[36] Specifically, this macrophage-derived nitric oxide may diffuse into the cartilage matrix and activate the Notch signaling pathway in resident chondrocytes. Inhibiting nitric oxide production in synovial macrophages or targeting the Notch-driven M1 polarization therefore provides a pharmacological strategy to prevent pathological Notch activation in arthritis.[31,37] In human osteoarthritis, high nitric oxide levels inhibit matrix synthesis and accelerate matrix breakdown.[1] Therefore, we used the NO donor sodium nitroprusside (SNP)[3] to establish OA chondrocyte injury cell model. In vitro, SNP increased *iNOS* in C28 cells, suppressed matrix synthesis, and promoted catabolism. Crucially, we found that NO activated Notch signaling. While the NO-Notch activation cascade is well-known in tumors[11–13] and heart disease,[38] its role in chondrocytes is rarely reported.

Notch signaling regulates tissue development and homeostasis,[7] including in osteoarthritis and cartilage.[6] However, its role in OA is complex.[8] While physiological Notch signaling helps maintain the joint,[8,39,40] sustained activation leads to promote OA pathology progression.[8–10] We found that exogenous NO caused sustained Notch activation in C28 cells, driving cartilage degeneration. Mechanistically, Notch activation releases the intracellular domain (NICD), which enters the nucleus to activate Hes1.[7] Hes1 binds the cofactor CaMK2δ, switching from a repressor to an activator. This increases cartilage catabolic factors and IL-6,[41,42] degrading the matrix and triggering inflammation. Moreover, Notch creates a feedback loop with the inflammatory NF-κB pathway. NF-κB increases Notch ligands like Jagged1,[43] while Notch boosts IL-6.[41] This signaling feedback enhances inflammation and NF-κB activation, and sustained Notch signaling thereby perpetuates cartilage degradation. This means simply blocking inflammation might fail due to Notch continually reactivates NF-κB. Targeting downstream effectors such as the Hes1–CaMK2δ interaction or administering DAPT can effectively disrupt this sustained signaling cycle. Previous studies show that DAPT reduces Jagged1, Hes1, and MMP13,[9,10] and improves cartilage degeneration[10] and knee pain in OA mice.[44] These findings align with our results.

While downstream Notch effectors in OA are well-characterized, the mechanism coupling the inflammatory NO burst to pathological Notch activation remains unclear. Here, we identify Gucy1a3 as a critical regulatory molecule in osteoarthritis pathology. While previous studies evaluated Gucy1a3 primarily in cardiovascular physiology,[18,19] our findings delineate its specific function within articular cartilage. In chondrocytes, Gucy1a3 mediates nitric oxide signaling to activate the Notch pathway. This observation updates conventional models where Notch activation requires cell-to-cell contact.[13,45] Gucy1a3 enables diffusible nitric oxide to activate Notch signaling in chondrocytes independent of cellular physical interactions.[13] Our data support the existence of a reciprocal positive feedback loop between Gucy1a3 and Notch signaling, rather than a simple unidirectional pathway. First, knockdown of *Gucy1a3* significantly inhibited the SNP-induced *Notch1* and *Jagged1* increase, confirming that Gucy1a3 is required for the initiation of Notch signaling; Second, we identified a feedback regulation where Notch maintains *Gucy1a3* expression. Since DAPT is a specific γ-secretase inhibitor that does not directly target sGC enzymes, the observed suppression of *Gucy1a3* mRNA following DAPT treatment is a consequence of inhibited Notch transcriptional activity. This pharmacological evidence aligns with established cardiovascular models demonstrating that *Gucy1a3* functions as a direct transcriptional target of Notch, with Notch activation upregulating sGC expression via RBPJ-dependent mechanisms.[15] Biologically, this reciprocal activation creates a self-sustaining cycle: an initial NO trigger activates Gucy1a3, and the resulting Notch signaling maintains high *Gucy1a3* transcription. This positive feedback loop prevents the resolution of inflammation, progressively sensitizing chondrocytes to the catabolic microenvironment and driving persistent matrix degradation. Although Gucy1a3 knockdown reduced SNP-driven Notch signaling and reduced IL-6 and ADAMTS5 expression, it did not rescue the decline in ACAN and Collagen II. This finding indicates that the NO-Gucy1a3-Notch axis functions predominantly to promote catabolism and inflammation rather than to inhibit anabolism. Consequently, Gucy1a3 knockdown mitigates the inflammatory response and limits damage but is insufficient to restore matrix synthesis.

Compared to Gucy1a3 knockdown, DAPT treatment resulted in higher expression of Collagen II and ACAN proteins. Because Gucy1a3 knockdown alone was insufficient to fully recover these matrix components, the effects of DAPT likely extend beyond the inhibition of Gucy1a3-mediated catabolism to support anabolic processes. By inhibiting γ-secretase, DAPT relieves Notch-mediated suppression of differentiation, providing a pharmacological basis for cartilage repair.

This pharmacological release of differentiation suppression extends beyond mature chondrocytes to encompass a multi-cellular therapeutic mechanism within the osteoarthritic joint. In our study, DAPT robustly promoted the chondrogenic differentiation of rat BMSCs, evidenced by the formation of larger, more numerous cartilage pellets.

Consistent with this, established literature demonstrates that Notch activation inhibits the osteogenic differentiation of mesenchymal stem cells,[28,30] and DAPT treatment effectively relieves this suppression to promote osteogenesis[30] and prevent inflammation-mediated bone loss.[28] Furthermore, Notch signaling restricts the osteogenic differentiation of committed osteoblastic cells (eg, MC3T3-E1),[25–27,30] and pharmacological inhibition with DAPT promotes the osteogenic maturation of these pre-osteoblasts.[30] Therefore, by removing the Notch-mediated barrier to differentiation, DAPT simultaneously enhances cartilage matrix synthesis, stimulates BMSC chondrogenesis, and normalizes subchondral osteoblast function.

This suggests that endogenous Notch signaling maintains the undifferentiated state and restricts lineage commitment under inductive conditions until the pathway is inhibited. Mechanistically, this effect likely stems from the disruption of stemness maintenance. Constitutive Notch activity is a well-established requirement for preserving MSC self-renewal and developmental plasticity, preventing premature differentiation.[46–48] Conversely, Notch blockade forces stem cells out of quiescence, triggering spontaneous lineage entry.[49] In our model, DAPT inhibits Notch signaling to promote the exit of BMSCs from the undifferentiated state and enhance chondrogenic differentiation.

A parallel regulatory logic governs osteogenesis. As described in the two-phase action model, early-stage Notch activation acts as a brake, inhibiting the transition from MSC to osteoprogenitor.[50] Previous research identified the molecular basis for this, demonstrating that Notch represses master transcription factors (eg, Runx2) via Hes/Hey proteins.[51] Previous studies indicate that the downregulation of Notch signaling at specific stages is required for the transition of stem cells into differentiated cells.[52,53] Our data imply DAPT removes an analogous early-stage barrier in chondrogenesis, potentially relieving the suppression of key drivers like Sox9.

The capacity of DAPT to promote differentiation by depleting stemness is further validated in cancer models, where $\gamma$-secretase inhibition reverses the undifferentiated phenotype by sharply downregulating core stemness factors, including Oct4, Sox2, and CD44.[54,55] While prior literature has predominantly focused on osteogenic differentiation[50–53] or malignancy,[54,55] our findings revealed a specific negative regulatory role for Notch at the initiation stage of chondrogenesis. We demonstrate that DAPT promotes differentiation and provides a pharmacological strategy to optimize seed cells for cartilage tissue engineering.

Despite these promising findings, several limitations warrant consideration. First, the sample size of three independent biological replicates used for in vitro molecular assays restricts statistical power, even though this small cohort aligns with standard practices for controlled cell-based studies with low anticipated biological variance. Furthermore, our in vitro mechanistic investigations rely primarily on a single immortalized human chondrocyte cell line. Although our initial phenotypic validations confirm that C28/I2 cells robustly upregulate catabolic markers and activate the Notch pathway in response to sodium nitroprusside, immortalized cell lines may not fully capture the complex pathophysiological responses of primary human articular chondrocytes. Although we evaluated our findings using nonparametric bootstrap resampling that proved scientific rationality, these in vitro results must be interpreted cautiously. Consequently, further validation in larger and more diverse experimental systems, including primary patient-derived chondrocytes and longer-term translational models, is essential to confirm the broad generalizability of the Gucy1a3 and Notch axis. Second, although we identified the interaction between Gucy1a3 and Notch using DAPT and siRNA knockdown, the exact transcriptional mechanism underlying the feedback regulation of Gucy1a3 by Notch signaling requires direct validation. Future studies using chromatin immunoprecipitation are necessary to determine whether the Notch intracellular domain binds directly to the Gucy1a3 promoter or acts through intermediate effectors such as Hes or Hey. Third, although our in vivo rat model successfully demonstrated the therapeutic efficacy of DAPT, the long-term safety profile of intra-articular Notch inhibition, particularly regarding potential off-target effects on synovial homeostasis or stem cell maintenance in the niche, requires more extensive longitudinal evaluation. Additionally, the medial meniscectomy model induces mild to moderate osteoarthritis. Testing DAPT in the severe anterior cruciate ligament transection model is necessary to confirm its broad efficacy. Nevertheless, this study serves as a foundational step, establishing the NO-Gucy1a3-Notch axis as a viable therapeutic target. Furthermore, translating this pharmacological strategy may need to incorporate DAPT with cartilage-penetrating delivery systems. Because chondrocytes reside deep within an avascular extracellular matrix, utilizing cationic peptides or specific carrier proteins could improve drug penetration into the cartilage matrix and extends local therapeutic efficacy.[56,57] Our ongoing work aims to develop more specific Gucy1a3 inhibitors or localized delivery systems to refine this strategy for clinical OA treatment translation.

## Conclusion

In conclusion, our findings identify the NO-Gucy1a3-Notch signaling axis as a key molecular driver of osteoarthritis pathology. Gucy1a3 transduces soluble nitric oxide signals to activate the Notch pathway. Pharmacological inhibition with DAPT provides therapeutic benefits across multiple cell types in the joint. DAPT decreases catabolism and promotes anabolism in chondrocytes, stimulates the chondrogenic and osteogenic differentiation of mesenchymal stem cells, and promotes osteogenic differentiation in subchondral osteoblasts. Modulating this pathway provides a pharmacological basis for developing osteoarthritis treatments that simultaneously address cartilage degradation, impaired regeneration, and subchondral bone remodeling.

## Abbreviations

OA, Osteoarthritis; NO, Nitric oxide; SNP, sodium nitroprusside; BMSCs, bone marrow mesenchymal stem cells; sGC, soluble guanylate cyclase; BV/TV, Bone Volume/Tissue Volume; BS/TV, Bone Surface area/Tissue Volume; Tb.N, Trabecular Number; Tb.Th, Trabecular Thickness; Tb.Sp, Trabecular Separation; Tb.Pf, Trabecular Pattern Factor.

## Acknowledgments

During the preparation of this work the authors used Gemini 3 Pro Preview in order to improve the grammatical accuracy and flow of the text. This tool was used solely for language refinement and did not replace human critical thinking, professional expertise, or scientific evaluation; it was employed under the strict supervision and control of the authors. After using this tool, the authors reviewed and edited the content as needed and take full responsibility for the content of the published article.

## Author Contributions

All authors made a significant contribution to the work reported, whether that is in the conception, study design, execution, acquisition of data, analysis and interpretation, or in all these areas; took part in drafting, revising or critically reviewing the article; gave final approval of the version to be published; have agreed on the journal to which the article has been submitted; and agree to be accountable for all aspects of the work.

## Funding

This work was supported by grants from the National Natural Science Foundation of China (No. 81703584), Guangdong Basic and Applied Basic Research Foundation (No. 2022A1515220166, 2025A1515010196, 2023A1515011091), Administration of Traditional Chinese Medicine of Guangdong Province, China (No.20250047), the Science and Technology Foundation of Zhanjiang (No. 2022A01099, 2022A01163), the Discipline Construction Fund of Central People's Hospital of Zhanjiang (No. 2022A09).

## Disclosure

The authors declare that there are no conflicts of interest in this work.

## References

1. Scher JU, Pillinger MH, Abramson SB. Nitric oxide synthases and osteoarthritis. *Curr Rheumatol Rep*. 2007;9(1):9–15. doi:10.1007/s11926-007-0016-z
2. Santoro A, Conde J, Scotece M, et al. Choosing the right chondrocyte cell line: focus on nitric oxide. *J Orthopaedic Res*. 2015;33(12):1784–1788. doi:10.1002/jor.22954
3. Quan YY, Qin GQ, Huang H, Liu YH, Wang XP, Chen TS. Dominant roles of Fenton reaction in sodium nitroprusside-induced chondrocyte apoptosis. *Free Radic Biol Med*. 2016;94:135–144. doi:10.1016/j.freeradbiomed.2016.02.026
4. Yu XB, Chen GY, Zhou L, et al. Chondroprotective effects of gubitong recipe via inhibiting excessive mitophagy of chondrocytes. *Evidence Based Complement Alternat Med*. 2022;2022:8922021. doi:10.1155/2022/8922021
5. Chen GY, Liu XY, Chen JQ, et al. Prediction of rhizoma drynariae targets in the treatment of osteoarthritis based on network pharmacology and experimental verification. *Evidence Based Complement Alternat Med*. 2021;2021:5233462. doi:10.1155/2021/5233462
6. Minguzzi M, Panichi V, D'Adamo S, et al. Pleiotropic roles of NOTCH1 signaling in the loss of maturational arrest of human osteoarthritic chondrocytes. *Int J Mol Sci*. 2021;22(21). doi:10.3390/ijms222112012

7. Zhou B, Lin W, Long Y, et al. Notch signaling pathway: architecture, disease, and therapeutics. *Signal Transduction Targeted Ther*. 2022;7(1):95. doi:10.1038/s41392-022-00934-y
8. Liu Z, Chen J, Mirando AJ, et al. A dual role for NOTCH signaling in joint cartilage maintenance and osteoarthritis. *Sci Signaling*. 2015;8(386): ra71. doi:10.1126/scisignal.aaa3792
9. Sassi N, Gadgadi N, Laadhar L, et al. Notch signaling is involved in human articular chondrocytes de-differentiation during osteoarthritis. *J Receptor Signal Transduction Res*. 2014;34(1):48–57. doi:10.3109/10799893.2013.856920
10. Hosaka Y, Saito T, Sugita S, et al. Notch signaling in chondrocytes modulates endochondral ossification and osteoarthritis development. *Proc Natl Acad Sci USA*. 2013;110(5):1875–1880. doi:10.1073/pnas.1207458110
11. Ishimura N, Bronk SF, Gores GJ. Inducible nitric oxide synthase up-regulates Notch-1 in mouse cholangiocytes: implications for carcinogenesis. *Gastroenterology*. 2005;128(5):1354–1368. doi:10.1053/j.gastro.2005.01.055
12. Zhang T, Lei J, Zheng M, Wen Z, Zhou J. Nitric oxide facilitates the S-nitrosylation and deubiquitination of Notch1 protein to maintain cancer stem cells in human NSCLC. *J Cell Mol Med*. 2024;28(21):e70203. doi:10.1111/jcmm.70203
13. Charles N, Ozawa T, Squatrito M, et al. Perivascular nitric oxide activates notch signaling and promotes stem-like character in PDGF-induced glioma cells. *Cell Stem Cell*. 2010;6(2):141–152. doi:10.1016/j.stem.2010.01.001
14. Kopan R, Ilagan MX. The canonical Notch signaling pathway: unfolding the activation mechanism. *Cell*. 2009;137(2):216–233. doi:10.1016/j.cell.2009.03.045
15. Rippe C, Zhu B, Krawczyk KK, et al. Hypertension reduces soluble guanylyl cyclase expression in the mouse aorta via the Notch signaling pathway. *Sci Rep*. 2017;7(1):1334. doi:10.1038/s41598-017-01392-1
16. Kessler M, Hoffmann K, Brinkmann V, et al. The Notch and Wnt pathways regulate stemness and differentiation in human fallopian tube organoids. *Nat Commun*. 2015;6:8989. doi:10.1038/ncomms9989
17. Yan B, Lu Q, Gao T, et al. CD146 regulates the stemness and chemoresistance of hepatocellular carcinoma via JAG2-NOTCH signaling. *Cell Death Dis*. 2025;16(1):150. doi:10.1038/s41419-025-07470-x
18. Kosmac K, Ismaeel A, Kim-Shapiro DB, McDermott MM. Praliciguat and soluble guanylate cyclase stimulators for peripheral artery disease. *Circul Res*. 2023;132(1):49–51. doi:10.1161/circresaha.122.322298
19. Butler J, Usman MS, Anstrom KJ, et al. Soluble guanylate cyclase stimulators in patients with heart failure with reduced ejection fraction across the risk spectrum. *Eur J Heart Failure*. 2022;24(11):2029–2036. doi:10.1002/ejhf.2720
20. Andersson ER, Lendahl U. Therapeutic modulation of Notch signalling--are we there yet? *Nat Rev Drug Discov*. 2014;13(5):357–378. doi:10.1038/nrd4252
21. Pang D, Laferriere C. Review of intraperitoneal injection of sodium pentobarbital as a method of euthanasia in laboratory rodents. *J Am Assoc Lab Animal Sci*. 2020;59(3):346. doi:10.30802/aalas-jaalas-19-000081
22. American Veterinary Medical Association. *AVMA Guidelines for the Euthanasia of Animals: 2020 Edition*. 2020. Available from: https://www.avma.org/sites/default/files/2020-02/Guidelines-on-Euthanasia-2020.pdf. Accessed May 08, 2026.
23. Wang S, Ma J, Zhao X, et al. The osteoarthritis natural progress and changes in intraosseous pressure of the Guinea pig model in different degeneration stages. *Orthopaedic Surg*. 2022;14(11):3036–3046. doi:10.1111/os.13496
24. Go EJ, Kim SA, Cho ML, Lee KS, Shetty AA, Kim SJ. A combination of surgical and chemical induction in a rabbit model for osteoarthritis of the knee. *Tissue Eng Regen Med*. 2022;19(6):1377–1388. doi:10.1007/s13770-022-00488-8
25. Resuela-González JL, González-Gómez MJ, Rodríguez-Cano MM, et al. NOTCH1, 2, and 3 receptors enhance osteoblastogenesis of mesenchymal C3H10T1/2 cells and inhibit this process in preosteoblastic MC3T3-E1cells. *Different Res Biol Divers*. 2025;142:100837. doi:10.1016/j.diff.2025.100837
26. Rong X, Kou Y, Zhang Y, et al. ED-71 prevents glucocorticoid-induced osteoporosis by regulating osteoblast differentiation via notch and Wnt/β-catenin pathways. *Drug Des Devel Ther*. 2022;16:3929–3946. doi:10.2147/dddt.S377001
27. Ni J, Yuan XM, Yao Q, Peng LB. OSM is overexpressed in knee osteoarthritis and Notch signaling is involved in the effects of OSM on MC3T3-E1cell proliferation and differentiation. *IntJ Mol Med*. 2015;35(6):1755–1760. doi:10.3892/ijmm.2015.2168
28. Zhang H, Hilton MJ, Anolik JH, et al. NOTCH inhibits osteoblast formation in inflammatory arthritis via noncanonical NF-κB. *J Clin Invest*. 2014;124(7):3200–3214. doi:10.1172/jci68901
29. Lories RJ, Luyten FP. The bone-cartilage unit in osteoarthritis. *Nat Rev Rheumatol*. 2011;7(1):43–49. doi:10.1038/nrrheum.2010.197
30. Xu Y, Li L, Tang Y, Yang J, Jin Y, Ma C. Icariin promotes osteogenic differentiation by suppressing Notch signaling. *Eur J Pharmacol*. 2019;865:172794. doi:10.1016/j.ejphar.2019.172794
31. Sun W, Zhang H, Wang H, et al. Targeting notch-activated M1 macrophages attenuates joint tissue damage in a mouse model of inflammatory arthritis. *J Bone Mineral Res*. 2017;32(7):1469–1480. doi:10.1002/jbmr.3117
32. Chen J, Li F, Su Z, et al. Coupling regulation the pyroptosis and polarization of macrophage: novel insights into the pathogenesis and immunotherapy of osteoarthritis. *Tissue Cell*. 2026;99:103302. doi:10.1016/j.tice.2025.103302
33. Fujii J, Osaki T. Involvement of nitric oxide in protecting against radical species and autoregulation of M1-polarized macrophages through metabolic remodeling. *Molecules*. 2023;28(2). doi:10.3390/molecules28020814
34. Abramowitz LK, Hanover JA. Chronically Elevated O-GlcNAcylation Limits Nitric Oxide Production and Deregulates Specific Pro-Inflammatory Cytokines. *Front Immunol*. 2022;13:802336. doi:10.3389/fimmu.2022.802336
35. Kang JH, Kim JH, Gim JA, Lee MY. iNOS in macrophage polarization: pharmacological and regulatory insights. *Int J Mol Sci*. 2025;26(24). doi:10.3390/ijms262412056
36. Zhao K, Ruan J, Nie L, Ye X, Li J. Effects of synovial macrophages in osteoarthritis. *Front Immunol*. 2023;14:1164137. doi:10.3389/fimmu.2023.1164137
37. Rath M, Müller I, Kropf P, Closs EI, Munder M. Metabolism via Arginase or Nitric Oxide Synthase: two Competing Arginine Pathways in Macrophages. *Front Immunol*. 2014;5:532. doi:10.3389/fimmu.2014.00532
38. Bosse K, Hans CP, Zhao N, et al. Endothelial nitric oxide signaling regulates Notch1 in aortic valve disease. *J Mol Cell Cardiol*. 2013;60:27–35. doi:10.1016/j.yjmcc.2013.04.001
39. Mirando AJ, Liu Z, Moore T, et al. RBP-Jκ-dependent notch signaling is required for murine articular cartilage and joint maintenance. *Arthritis Rheum*. 2013;65(10):2623–2633. doi:10.1002/art.38076

40. Liu Z, Ren Y, Mirando AJ, et al. Notch signaling in postnatal joint chondrocytes, but not subchondral osteoblasts, is required for articular cartilage and joint maintenance. *Osteoarthritis Cartilage*. 2016;24(4):740–751. doi:10.1016/j.joca.2015.10.015
41. Sugita S, Hosaka Y, Okada K, et al. Transcription factor Hes1 modulates osteoarthritis development in cooperation with calcium/calmodulin-dependent protein kinase 2. *Proc Natl Acad Sci USA*. 2015;112(10):3080–3085. doi:10.1073/pnas.1419699112
42. Jiang L, Lin J, Zhao S, et al. ADAMTS5 in osteoarthritis: biological functions, regulatory network, and potential targeting therapies. *Front Mol Biosci*. 2021;8:703110. doi:10.3389/fmolb.2021.703110
43. Saito T, Tanaka S. Molecular mechanisms underlying osteoarthritis development: notch and NF-κB. *Arthritis Res Ther*. 2017;19(1):94. doi:10.1186/s13075-017-1296-y
44. Wang L, Ishihara S, Li J, Miller RE, Malfait AM. Notch signaling is activated in knee-innervating dorsal root ganglia in experimental models of osteoarthritis joint pain. *Arthritis Res Ther*. 2023;25(1):63. doi:10.1186/s13075-023-03039-1
45. Andersen P, Uosaki H, Shenje LT, Kwon C. Non-canonical notch signaling: emerging role and mechanism. *Trends Cell Biol*. 2012;22(5):257–265. doi:10.1016/j.tcb.2012.02.003
46. Cheng JW, Duan LX, Yu Y, et al. Bone marrow mesenchymal stem cells promote prostate cancer cell stemness via cell-cell contact to activate the Jagged1/Notch1 pathway. *Cell Biosci*. 2021;11(1):87. doi:10.1186/s13578-021-00599-0
47. Yang J, Hu Y, Wang L, Sun X, Yu L, Guo W. Human umbilical vein endothelial cells derived-exosomes promote osteosarcoma cell stemness by activating Notch signaling pathway. *Bioengineered*. 2021;12(2):11007–11017. doi:10.1080/21655979.2021.2005220
48. Shu Q, Zhuang H, Fan J, Wang X, Xu G. Wogonin induces retinal neuron-like differentiation of bone marrow stem cells by inhibiting Notch-1 signaling. *Oncotarget*. 2017;8(17):28431–28441. doi:10.18632/oncotarget.16085
49. Estupiñán Ó, Rey V, Tornín J, et al. Abrogation of stemness in osteosarcoma by the mithramycin analog EC-8042 is mediated by its ability to inhibit NOTCH-1 signaling. *Biomed Pharmacothe*. 2023;162:114627. doi:10.1016/j.biopha.2023.114627
50. Ji Y, Ke Y, Gao S. Intermittent activation of notch signaling promotes bone formation. *Am J Transl Res*. 2017;9(6):2933–2944.
51. Hilton MJ, Tu X, Wu X, et al. Notch signaling maintains bone marrow mesenchymal progenitors by suppressing osteoblast differentiation. *Nat Med*. 2008;14(3):306–314. doi:10.1038/nm1716
52. Uribe-Etxebarria V, Pineda JR, García-Gallastegi P, Agliano A, Unda F, Ibarretxe G. Notch and Wnt signaling modulation to enhance DPSC stemness and therapeutic potential. *Int J Mol Sci*. 2023;24(8). doi:10.3390/ijms24087389
53. Gao J, Fan L, Zhao L, Su Y. The interaction of Notch and Wnt signaling pathways in vertebrate regeneration. *Cell Regen*. 2021;10(1):11. doi:10.1186/s13619-020-00072-2
54. Jiang LY, Zhang XL, Du P, Zheng JH. γ-secretase inhibitor, DAPT inhibits self-renewal and stemness maintenance of ovarian cancer stem-like cells in vitro. *Chin J Cancer Res*. 2011;23(2):140–146. doi:10.1007/s11670-011-0140-1
55. Fender AW, Nutter JM, Fitzgerald TL, Bertrand FE, Sigounas G. Notch-1 promotes stemness and epithelial to mesenchymal transition in colorectal cancer. *J Cell Biochem*. 2015;116(11):2517–2527. doi:10.1002/jcb.25196
56. Bajpayee AG, Grodzinsky AJ. Cartilage-targeting drug delivery: can electrostatic interactions help? *Nat Rev Rheumatol*. 2017;13(3):183–193. doi:10.1038/nrrheum.2016.210
57. Morici L, Allémann E, Rodríguez-Nogales C, Jordan O. Cartilage-targeted drug nanocarriers for osteoarthritis therapy. *Int J Pharm*. 2024;666:124843. doi:10.1016/j.ijpharm.2024.124843